

Suppression of the antinodal coherence of superconducting $(\text{Bi,Pb})_2(\text{Sr,L a})_2\text{CuO}_{6+\delta}$ as revealed by muon spin rotation and angle-resolved photoemission

R. Khasanov,^{1,*} Takeshi Kondo,^{2,3} M. Bendele,^{1,4} Yoichiro Hamaya,³ A. Kaminski,² S. L. Lee,⁵ S. J. Ray,⁵ and Tsunehiro Takeuchi^{3,6}

¹Laboratory for Muon Spin Spectroscopy, Paul Scherrer Institute, CH-5232 Villigen PSI, Switzerland

²Ames Laboratory and Department of Physics and Astronomy, Iowa State University, Ames, Iowa 50011, USA

³Department of Crystalline Materials Science, Nagoya University, Nagoya 464-8603, Japan

⁴Physik-Institut der Universität Zürich, Winterthurerstrasse 190, CH-8057 Zürich, Switzerland

⁵School of Physics and Astronomy, University of St. Andrews, Fife KY16 9SS, United Kingdom

⁶EcoTopia Science Institute, Nagoya University, Nagoya 464-8603, Japan

(Received 10 June 2010; revised manuscript received 5 July 2010; published 22 July 2010)

The superfluid density ρ_s in underdoped ($T_c \approx 23$ K), optimally doped ($T_c \approx 35$ K), and overdoped ($T_c \approx 29$ K) single-crystalline $(\text{Bi,Pb})_2(\text{Sr,L a})_2\text{CuO}_{6+\delta}$ samples was studied by means of muon spin rotation (μSR). By combining the μSR data with the results of angle-resolved photoemission spectroscopy measurements on similar samples [T. Kondo *et al.*, *Nature (London)* **457**, 296 (2009)] good self-consistent agreement is obtained between two techniques concerning the temperature and the doping evolution of ρ_s .

DOI: 10.1103/PhysRevB.82.020511

PACS number(s): 74.72.Gh, 74.25.Jb, 76.75.+i, 79.60.-i

The superfluid density ρ_s , being proportional to the density of the supercarriers, is one of the important characteristic of the superconducting condensate. Considering that superconductivity is characterized by the phase coherence of electrons forming the pairs (two-particle process), it was previously believed that techniques which probe the single-particle excitations of the condensate, such as photoemission and single-electron tunneling, could not directly provide the information on ρ_s . It was quite unexpected, therefore, when angle-resolved photoemission spectroscopy (ARPES) studies of the cuprate high-temperature superconductor (HTS) $\text{Bi}_2\text{Sr}_2\text{CaCu}_2\text{O}_{8+\delta}$ revealed that a sharp peak, formed below the superconducting transition temperature T_c near the Brillouin-zone boundary, contains information not only on the pairing strength (the superconducting energy gap Δ) but also on the phase coherence.¹ The peak intensity shows a clear resemblance to the behavior exhibited by ρ_s and scales linearly with T_c in the underdoped regime.¹

The previous comparisons between ρ_s and the coherence peak (CP) were made for CP measured near the Brillouin-zone boundary.¹ The superfluid density, in its turn, is an “angular integrated” quantity accumulating information over the full Fermi surface. More importantly, the carriers near the antinodes could be affected by the pseudogap, which within the “two-gap” scenario is unrelated to the pairing.^{2–4} This could lead to an additional decrease in the CP intensity in the antinodal region.⁴ Consequently the CP measurements over the full Brillouin zone are needed in order to compare ARPES data with ρ_s studied independently in, e.g., muon spin rotation (μSR) or microwave experiments.

In this Rapid Communication we report on the results of μSR studies of the superfluid density and its comparison with the previously reported ARPES data⁴ for underdoped ($T_c \approx 23$ K), optimally doped ($T_c \approx 35$ K), and overdoped ($T_c \approx 29$ K) single-crystalline $(\text{Bi,Pb})_2(\text{Sr,L a})_2\text{CuO}_{6+\delta}$ ($\text{Bi}2201$) samples. It was found that $\rho_s(T)$ could be well described with a superconducting gap of d -wave symmetry by introducing the coherence quasiparticle weight function (QW) measured by means of ARPES. The T dependence of

the superconducting energy gap Δ follows the BCS prediction and ρ_s scales with the CP intensity integrated over the whole Fermi surface.

Details on the sample preparation of $(\text{Bi,Pb})_2(\text{Sr,L a})_2\text{CuO}_{6+\delta}$ single crystals can be found elsewhere.^{4,5} The samples are labeled by their T_c 's with the prefix UD for underdoped, OP for optimally doped, and OD for overdoped as: UD23K, OP35K, and OD29K. Zero-field (ZF) and transverse-field (TF) μSR experiments were carried out at the $\pi M3$ beamline (Paul Scherrer Institute, Switzerland). The samples were cooled from above T_c to 1.6 K at $H=0$ during ZF and in a series of fields ranging from 5 mT to 0.64 T in TF- μSR experiments. In TF studies the magnetic field was applied parallel to the c axis and transverse to the muon spin polarization. The typical counting statistics were 15–18 million muon detections per data point. The TF- μSR data for OP35K are partially presented in Refs. 6 and 7.

The representative ZF and TF- μSR time spectra measured above and below T_c are shown in the left panels of Figs. 1(a)–1(c). In ZF all three samples show a slow, temperature-independent decay thus implying that the T -dependent relaxation observed in TF experiments at $T < T_c$ should be attributed to the inhomogeneous field distribution in a superconductor in the vortex state. The ZF data for OP35K and OD29K are well described by the Gaussian decay function $A^{\text{ZF}}(t) = A_0 \exp(-\sigma_G^2 t^2/2)$ which is caused by the dipolar field arising from the nuclear magnetic moments (A_0 is the initial asymmetry and σ_G is the Gaussian depolarization rate). The exponential character of the muon polarization decay in UD23K, described as $A^{\text{ZF}}(t) = A_0 \exp(-\Lambda t)$, is an indication of a weak magnetism which is probably caused by the closed proximity to the static magnetic order.⁸

The TF- μSR data were analyzed by using a two-component Gaussian fit of the μSR time spectra allowing to describe the asymmetric local magnetic field distribution $P(B)$ in a superconductor in the vortex state: $A^{\text{TF}}(t) = \sum_{i=1}^2 A_i \exp(-\sigma_i^2 t^2/2) \cos(\gamma_\mu B_i t + \varphi)$.^{6,9,10} Here A_i , σ_i , and B_i are the initial asymmetry, relaxation rate, and mean field of the i th component, $\gamma_\mu = 2\pi \times 135.5342$ MHz/T is

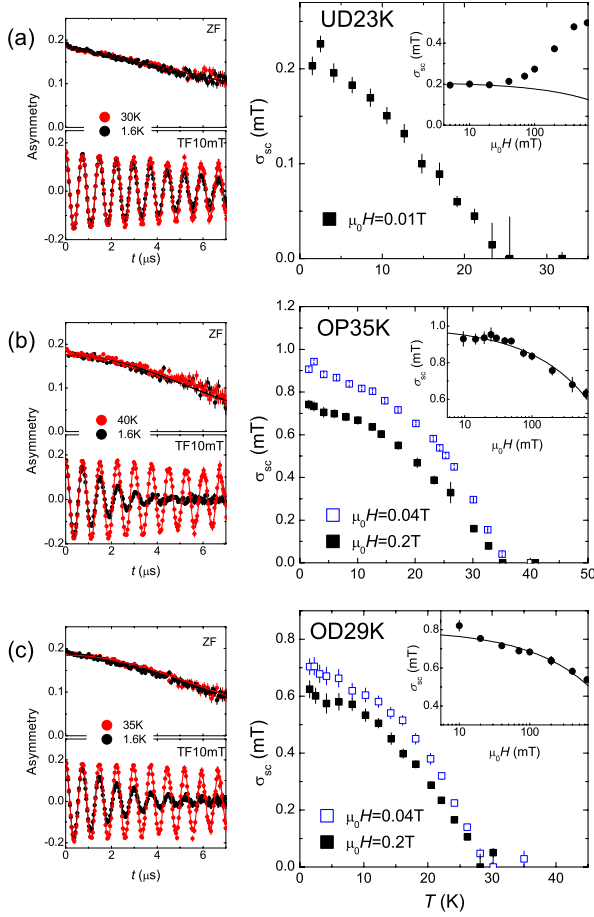


FIG. 1. (Color online) The representative ZF and TF- μ SR time spectra measured above and below T_c (left panels), and the dependence of $\sigma_{sc} \propto \lambda_{ab}^{-2} \propto \rho_s$ on temperature and magnetic field (right panels) for (a) UD23K, (b) OP35K, and (c) OD29K.

the muon gyromagnetic ratio, and φ is the initial phase of the muon spin ensemble. The weak magnetism detected in ZF experiments for UD23K was taken into account by multiplying the fitting function by $\exp(-\Lambda t)$. The superconducting part of the square root of the second moment $\sigma_{sc} \propto \lambda_{ab}^{-2} \propto \rho_s$ (λ_{ab} is the in-plane magnetic penetration depth) was further obtained by subtracting the normal-state nuclear moment contribution (σ_{nm}) from the measured second moment of $P(B)$ (σ^2) as $\sigma_{sc} = \sqrt{\sigma^2 - \sigma_{nm}^2}$.^{9,10}

The magnetic field dependence of σ_{sc} at $T = 1.6$ K for the samples studied is shown in the corresponding insets of Figs. 1(a)–1(c). The decrease in σ_{sc} for OP35K and OD29K is a consequence of both, the nonlinear and the nonlocal response of the superconductor containing nodes in the energy gap to the increasing magnetic field.⁷ The solid lines for OD29K and OP35K correspond to fits of the relation $\sigma_{sc}(H)/\sigma_{sc}(H=0) = 1 - K \cdot \sqrt{H}$ to $\sigma_{sc}(H)$ which takes into account the nonlinear correction to ρ_s for a superconductor with a d -wave energy gap.¹¹ The analysis of $\sigma_{sc}(H)$ for UD23K reveals, however, that only at very low fields (≤ 30 mT) σ_{sc} follows the tendency observed for OP and OD Bi2201 samples. For higher fields σ_{sc} increases with increasing H . Such behavior is generally associated with the field-induced magnetism and is often observed in various underdoped cuprate HTS (see, e.g., Ref. 12).

The observation of the field-induced magnetism in UD23K for fields exceeding 30 mT is quite unexpected, especially considering the fact that in their recent study Russo *et al.*⁸ do not detect any kind of field-induced effects in Bi2201 with $T_c \approx 27$ K up to $\mu_0 H \approx 5$ T. We may suggest, therefore, that the partial substitution of Bi by Pb, as made in our samples, leads to enhancement of coupling between CuO_2 layers, thus causing Bi2201 to be more three dimensional. This could affect both, the superconducting and the magnetic properties. As for superconductivity, our previous studies point to a substantial reduction in the anisotropy coefficient $\gamma_\lambda = \lambda_c/\lambda_{ab}$ (λ_c is the out-of-plane component of the magnetic penetration depth) as well as to the shift of the vortex-lattice melting transition much closer to T_c .⁶ The magnetic properties could be also affected due to increase in the interlayer magnetic exchange coupling J' , which for the layered materials like cuprate HTS is the primary quantity determining the Néel temperature $T_N \propto J' \xi_{2D}^2$ (ξ_{2D} is the magnetic correlation lengths within the layer).

The temperature dependence of λ_{ab} was obtained from the measured $\sigma_{sc}(H = \text{const}, T)$'s shown in Fig. 1 by following the procedure described in Ref. 7. It includes, first, the reconstruction of the effective penetration depth $\lambda_{eff}(H, T)$ from $\sigma_{sc}(H, T)$ by using the relation $\sigma_{sc}(H, T) = 4.83 \times 10^4 [1 - H/H_{c2}(T)] [1 + 1.21(1 - \sqrt{H/H_{c2}(T)})^3] \lambda_{eff}^{-2}$.¹³ Here H_{c2} is the upper critical field with the zero-temperature values $\mu_0 H_{c2}(0) \approx 60$ T, ≈ 50 T, and ≈ 45 T for UD23K, OP35K, and OD29K, respectively,¹⁴ and with the T dependence following the Werthamer-Helfand-Hohenberg (WHH) type of dependence as observed for Bi2201 at low temperatures¹⁶ is expected to play a minor role since the theory of Brandt¹³ considers the terms on the order of $[1 - H/H_{c2}(T)]$. As a next step, λ_{ab} was reconstructed by decomposing $\lambda_{eff}(H, T)$ into the field and the temperature-dependent components as $\lambda_{eff}(H/H_{c2}, T) = C(H/H_{c2}) \lambda_{ab}(T)$.

The dependence of $\lambda_{ab}^{-2} \propto \rho_s$ on temperature is shown in Fig. 2. For OP35K and OD29K $\lambda_{ab}^{-2}(T)$ was reconstructed from $\sigma_{sc}(H, T)$'s measured at $\mu_0 H = 0.04, 0.1, 0.2, 0.4,$ and 0.64 T (see Ref. 7), and $\mu_0 H = 0.04$ T and 0.2 T, respectively. The field-induced magnetism does not allow us to make a similar reconstruction for UD23K. We assumed, therefore, $\lambda_{ab}(T) \approx \lambda_{eff}(0.01 \text{ T}, T)$. As shown in Ref. 7 the relation $\lambda_{eff}(H, T) \approx \lambda_{ab}(T)$ is still valid in the limit of low magnetic fields $H \lesssim 10^{-3} H_{c2}(0)$.

The resulting $\lambda_{ab}^{-2}(T)$'s were analyzed within the same scheme as described in Refs. 6 and 7,

$$\frac{\lambda_{ab}^{-2}(T)}{\lambda_{ab}^{-2}(0)} = 1 + \frac{2}{S_{QW}} \int_0^{\pi/4} \int_{\Delta(T, \phi)}^{\infty} \left(\frac{\partial f}{\partial E} \right) \frac{QW(\phi) E dE d\phi}{\sqrt{E^2 - \Delta(T, \phi)^2}}. \quad (1)$$

Here $f = [1 + \exp(E/k_B T)]^{-1}$ is the Fermi function, ϕ is the angle along the Fermi surface [see the top right panels in Figs. 2(a)–2(c)], $\Delta(T, \phi)$ denotes the superconducting (pairing) gap depending on T and ϕ , $QW(\phi)$ accounts for the relative weight of the quasiparticles available for condensate, and $S_{QW} = \int_0^{\pi/4} QW(\phi) d\phi$. Note that we do not consider here the presence of the second s -wave gap^{10,17} since the d -wave contribution to $\lambda_{ab}^{-2}(T)$ in Bi2201 seems to be predominant.

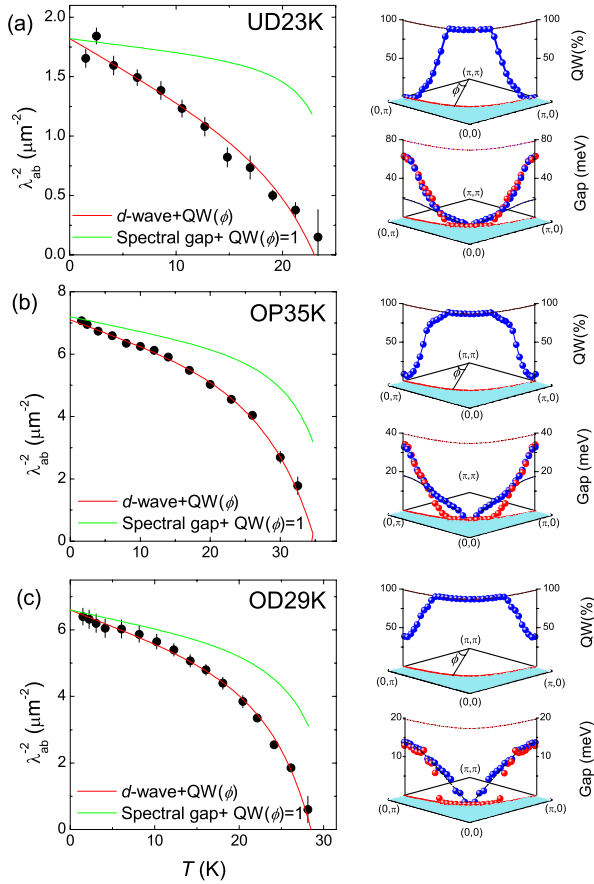


FIG. 2. (Color online) (a) The μ SR and ARPES data for UD23K sample. Left panel: $\lambda_{ab}^{-2}(T) \propto \rho_s(T)$. Lines are the theoretical $\lambda_{ab}^{-2}(T)$ obtained by assuming that the full spectral gap measured by means of ARPES leads to the pairing and $QW(\phi)=1$ (green line) and for the gap of d -wave symmetry with $QW(\phi)$ measured by ARPES (red line). Top right panel: angular dependence of the quasiparticle weight function $QW(\phi)$ (Ref. 4). $\phi=0$ and $\phi=\pi/4$ correspond to the antinodal and the nodal directions, respectively. Bottom right panel: angular dependence of the spectral gap above (41 K, red dots) and below (11 K, blue dots) $T_c \approx 23$ K (Ref. 4). The solid line is the $\cos 2\phi$ fit of $T=11$ K data in the nodal region. (b) and (c)—the same as in (a) but for OP35K and OD29K, respectively.

As a first step we checked if the full spectral gap measured in ARPES experiments [lower right panels in Figs. 2(a)–2(c)] could be a pairing gap. The solid green lines on the left panels of Figs. 2(a)–2(c) correspond to the theoretical curves obtained by assuming that the states over the whole Fermi surface are equally available for condensation [$QW(\phi)=1$], and that the gap in the antinodal region is T independent while it follows the BCS prediction close to the nodes.³ The poor agreement between the experiment and the theory suggests that the gap near the antinodes could not be related to the pairing. In particular, the steplike jump of ρ_s at $T=T_c$ is due to the fact that the antinodal gap is not closed when the temperature passes through T_c .

We suggest, therefore, that for all levels of doping the superconducting (pairing) gap has a d -wave symmetry: $\Delta(T, \phi) = \Delta(T) \cos 2\phi$. This is indeed true for OD29K (Fig. 2 and Ref. 4), as well as for various OD and OP hole-doped

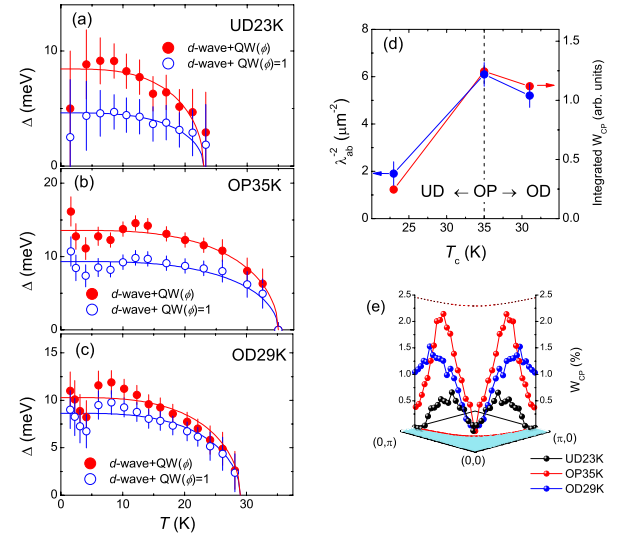


FIG. 3. (Color online) Temperature dependence of the superconducting gap for (a) UD23K, (b) OP35K, and (c) OD29K. The open and closed symbols correspond to $QW(\phi)=1$ and $QW(\phi)$ measured by means of ARPES (Ref. 4). The solid lines are BCS fits with parameters summarized in Table I. (d) Dependence of $\lambda_{ab}^{-2}(T=11$ K) and the coherence peak intensity W_{CP} integrated over the whole Fermi surface on T_c . (e) Angular dependence of W_{CP} measured by ARPES (Ref. 4).

cuprate HTS studied by means of ARPES (see, e.g., Ref. 18 and references therein). The predominantly d -wave symmetry of the order parameter in UD HTS was also confirmed in tricrystal experiments.¹⁹ This, together with known $QW(\phi)$ and $\lambda_{ab}^{-2}(T)$ allows the use of Eq. (1) to reconstruct $\Delta(T)$. The results of such reconstruction for two possible scenarios are shown in Fig. 3: the first with $QW(\phi) = W_{CP}/(W_{CP} + W_{PG})$ obtained by means of ARPES (see Fig. 2 and Refs. 4 and 20) and the second with $QW(\phi)=1$, as indicated by the closed and open symbols, respectively. Here W_{CP} is the intensity of the coherence peak and W_{PG} is the spectral weight loss in the pseudogap state (see Ref. 4 for details). Fits of the BCS model to $\Delta(T)$ are represented by solid lines. Both sets of $\Delta(T)$ data follow the BCS temperature dependence in agreement with the results of ARPES studies for the spectral gap in the nodal region.³

In order to distinguish between the two above-mentioned scenarios we note that: (i) accounting for the quasiparticle weight as measured by ARPES causes a systematic shift of $\Delta(T)$ to higher values. This leads to better agreement with the gap obtained from the $\cos 2\phi$ fit to the ARPES data in the nodal region.⁴ (ii) The ratio $2\Delta/k_B T_c$ increases with doping from ≈ 4.6 for UD23K to 6.9 for OD29K in a case when $QW(\phi)=1$ while it stays almost constant (~ 8.5) for $QW(\phi)$ obtained by means of ARPES, see Table I. Note that the independence of $2\Delta/k_B T_c$ ratio on doping is well confirmed experimentally for various HTS families (see, e.g., Ref. 21 and references therein). (iii) The intensity of the coherence peak W_{CP} [Fig. 3(e)] integrated over the whole Fermi surface scales with ρ_s [Fig. 3(d)], thus pointing to the direct relation of W_{CP} to the “local” density of the Cooper pairs (local superfluid density).^{1,4} By approaching the antinodal point W_{CP} decreases. The strongest effect (decrease in W_{CP} down to 0)

TABLE I. Zero-temperature values of the superconducting gap $\Delta(0)$ and the ratio $2\Delta(0)/k_B T_c$ as obtained from the fit of the BCS model to $\Delta(T)$ represented in Figs. 3(a)–3(c). The “*d*-wave” and “*d*-wave+QW(ϕ)” refer to the case of QW(ϕ)=1 and QW(ϕ) measured by means of ARPES (Ref. 4), respectively (see text for details). The last two columns are $T=11$ K values obtained in ARPES experiments (Ref. 4).

	<i>d</i> -wave		<i>d</i> -wave+QW(ϕ)		ARPES	
	$\Delta(0)$ (meV)	$2\Delta(0)/k_B T_c$	$\Delta(0)$ (meV)	$2\Delta(0)/k_B T_c$	$\Delta(11$ K) (meV)	$2\Delta(11$ K)/ $k_B T_c$
UD23K	4.6(2)	4.6(2)	8.4(3)	8.5(3)	19	19.2
OP35K	9.3(2)	6.2(1)	13.6(3)	9.0(2)	18	11.9
OD29K	8.6(2)	6.9(2)	10.3(3)	8.2(2)	14	11.2

is observed for UD23K while for OD29K the weight of CP in the nodal region still remains substantial. All these arguments taken together support the scenario according to which the gap (pseudogap) near the antinodes makes a part of the states unavailable for condensation and leads, therefore, to a reduced density of the supercarriers in the antinodal region.

To summarize, the temperature dependence of the superfluid density ρ_s was studied in underdoped ($T_c \approx 23$ K), optimally doped ($T_c \approx 35$ K), and overdoped ($T_c \approx 29$ K) single-crystalline Bi2201 samples by means of muon spin rotation. By comparing the measured $\rho_s(T)$ with that calculated theoretically based on the results of ARPES (Ref. 4) we found that the superconducting gap in Bi2201 at all levels of

doping has *d*-wave symmetry and that $\Delta(T)$ follows reasonably well the BCS prediction. It was also shown that $\rho_s(T)$ is inconsistent with the case when the carriers over the whole Fermi surface are equally available for condensation thus suggesting that some parts of the Fermi surface do not develop the superconducting coherence.

This work was performed at the Swiss Muon Source (Paul Scherrer Institute, Switzerland). Work at the Ames Laboratory was supported by the Department of Energy, Basic Energy Sciences under Contract No. DE-AC02-07CH11358. The financial support of the Swiss National Foundation (SNF) is gratefully acknowledged.

*Corresponding author; rustem.khasanov@psi.ch

¹D. L. Feng *et al.*, *Science* **289**, 277 (2000); H. Ding, J. R. Engelbrecht, Z. Wang, J. C. Campuzano, S. C. Wang, H. B. Yang, R. Rogan, T. Takahashi, K. Kadowaki, and D. G. Hinks, *Phys. Rev. Lett.* **87**, 227001 (2001).

²S. Chakravarty, R. B. Laughlin, D. K. Morr, and C. Nayak, *Phys. Rev. B* **63**, 094503 (2001); M. Le Tacon *et al.*, *Nat. Phys.* **2**, 537 (2006); K. Tanaka *et al.*, *Science* **314**, 1910 (2006); T. Kondo, T. Takeuchi, A. Kaminski, S. Tsuda, and S. Shin, *Phys. Rev. Lett.* **98**, 267004 (2007); T. Hanaguri *et al.*, *Nat. Phys.* **3**, 865 (2007); W. Guyard, M. Le Tacon, M. Cazayous, A. Sacuto, A. Georges, D. Colson, and A. Forget, *Phys. Rev. B* **77**, 024524 (2008); Y. Kohsaka *et al.*, *Nature (London)* **454**, 1072 (2008); T. Yoshida *et al.*, *Phys. Rev. Lett.* **103**, 037004 (2009); S. Blanc, Y. Gallais, A. Sacuto, M. Cazayous, M. A. Measson, G. D. Gu, J. S. Wen, and Z. J. Xu, *Phys. Rev. B* **80**, 140502(R) (2009).

³W. S. Lee *et al.*, *Nature (London)* **450**, 81 (2007).

⁴T. Kondo *et al.*, *Nature (London)* **457**, 296 (2009).

⁵T. Kondo *et al.*, *J. Electron Spectrosc. Relat. Phenom.* **137-140**, 663 (2004); T. Kondo, T. Takeuchi, U. Mizutani, T. Yokoya, S. Tsuda, and S. Shin, *Phys. Rev. B* **72**, 024533 (2005).

⁶R. Khasanov, T. Kondo, S. Strassle, D. O. G. Heron, A. Kaminski, H. Keller, S. L. Lee, and T. Takeuchi, *Phys. Rev. Lett.* **101**, 227002 (2008).

⁷R. Khasanov, T. Kondo, S. Strassle, D. O. G. Heron, A. Kaminski, H. Keller, S. L. Lee, and T. Takeuchi, *Phys. Rev. B* **79**, 180507(R) (2009).

⁸P. L. Russo *et al.*, *Phys. Rev. B* **75**, 054511 (2007).

⁹R. Khasanov *et al.*, *Phys. Rev. B* **72**, 104504 (2005); R. Khasanov, I. L. Landau, C. Baines, F. La Mattina, A. Mai-

suradze, K. Togano, and H. Keller, *ibid.* **73**, 214528 (2006).

¹⁰R. Khasanov, A. Shengelaya, A. Maisuradze, F. La Mattina, A. Bussmann-Holder, H. Keller, and K. A. Muller, *Phys. Rev. Lett.* **98**, 057007 (2007).

¹¹I. Vekhter, J. P. Carbotte, and E. J. Nicol, *Phys. Rev. B* **59**, 1417 (1999).

¹²A. T. Savici *et al.*, *Phys. Rev. B* **66**, 014524 (2002); R. Khasanov, N. D. Zhigadlo, J. Karpinski, and H. Keller, *ibid.* **76**, 094505 (2007).

¹³E. H. Brandt, *Phys. Rev. B* **68**, 054506 (2003).

¹⁴Y. Wang *et al.*, *Science* **299**, 86 (2003).

¹⁵N. R. Werthamer *et al.*, *Phys. Rev.* **147**, 295 (1966).

¹⁶S. I. Vedenev, C. Proust, V. P. Mineev, M. Nardone, and G. L. J. A. Rikken, *Phys. Rev. B* **73**, 014528 (2006).

¹⁷R. Khasanov, S. Strassle, D. Di Castro, T. Masui, S. Miyasaka, S. Tajima, A. Bussmann-Holder, and H. Keller, *Phys. Rev. Lett.* **99**, 237601 (2007); R. Khasanov *et al.*, *J. Supercond. Novel Magn.* **21**, 81 (2008).

¹⁸A. Damascelli *et al.*, *Rev. Mod. Phys.* **75**, 473 (2003).

¹⁹C. C. Tsuei, J. R. Kirtley, G. Hammerl, J. Mannhart, H. Raffy, and Z. Z. Li, *Phys. Rev. Lett.* **93**, 187004 (2004).

²⁰QW = $W_{CP}/(W_{CP}+W_{PG})$ may also depend on temperature as follows from $W_{PG}(T)$ shown in Fig. 1h of Ref. 4. Our numerical analysis reveals, however, that even 50% increase in W_{PG} does not affect the shape of QW(ϕ).

²¹R. Khasanov, S. Strassle, K. Conder, E. Pomjakushina, A. Bussmann-Holder, and H. Keller, *Phys. Rev. B* **77**, 104530 (2008); W. Guyard, A. Sacuto, M. Cazayous, Y. Gallais, M. Le Tacon, D. Colson, and A. Forget, *Phys. Rev. Lett.* **101**, 097003 (2008).